Ab initio theory of perpendicular magnetotransport in metallic multilayers

J. Kudrnovský,[1,2,4] V. Drchal,[1,2] C. Blaas,[2] P. Weinberger,[2] I. Turek,[2,3] and P. Bruno[4]
[1]*Institute of Physics, Academy of Sciences of the Czech Republic, Na Slovance 2, CZ-182 21 Prague 8, Czech Republic*
[2]*Center for Computational Materials Science, Technical University of Vienna, Getreidemarkt 9/158, A-1060 Vienna, Austria*
[3]*Institute of Physics of Materials, Academy of Sciences of the Czech Republic, Žižkova 22, CZ-616 62 Brno, Czech Republic*
[4]*Max-Planck-Institut für Mikrostrukturphysik, Weinberg 2, D-06120 Halle, Germany*
(Received 4 February 2000; revised manuscript received 13 June 2000)

The current-perpendicular-to-plane (CPP) magnetotransport of a metallic sample sandwiched by two ideal leads is described at an *ab initio* level. The so-called ''active'' part of the system is either a trilayer consisting of two magnetic slabs of finite thickness separated by a nonmagnetic spacer or a multilayer formed by alternating magnetic and nonmagnetic layers. We use a transmission matrix formulation of the conductance based on surface Green's functions as formulated by means of the tight-binding linear muffin-tin orbital method. The formalism is extended to the case of lateral supercells with random arrangements of atoms of two types, which in turn allows to deal with specular and diffusive scattering on equal footing, and which is applicable also to the case of noncollinear alignments of the magnetization in the layers. Applications refer to fcc-based Co/Cu/Co(001) trilayers and multilayers, considering in detail the effect of substitutional alloying in the spacer and in the magnetic layers, as well as interdiffusion at the interfaces.

I. INTRODUCTION

Transport in layered materials is subject of intensive theoretical investigations, in particular in view of the discovery of the giant magnetoresistance (GMR) in metallic multilayers.[1,2] Various theoretical approaches for a free-electron model or within a single-band tight-binding model have been proposed, based on the semiclassical Boltzmann equation or, alternatively, on a Kubo-Greenwood-type formulation with random point scatterers. A description of experimental and theoretical results can be found in a recent review article[3] (see also Ref. 4). Up to now the GMR effect has been observed mostly in the diffusive transport regime in which the mean free path is much smaller than the dimension of the so-called ''active'' part of the multilayer system, i.e., the whole system with exception of the leads. Most of the measurements up to date were performed in the current-in-plane (CIP) geometry;[1] the current-perpendicular-to-plane (CPP) geometry[2] seems to be experimentally more challenging. From a theoretical point of view CPP transport is interesting because of the obvious role played by interfaces, its close relation to tunneling across an insulator or vacuum, and because of its relation to a semiclassical view of ballistic transport.[5] The present theoretical understanding of the CPP transport has been reviewed in a recent paper,[6] including the transport in the ballistic regime. In this regime, in contrast to the diffusive regime, the mean free path is larger than the dimension of the active part of the multilayer system. Spin-dependent scattering at ideal interfaces between magnetic and nonmagnetic layers, the so-called intrinsic potential or specular scattering, is usually said to be the origin of the GMR in the ballistic regime.[5] In the diffusive regime the GMR is thought to originate from spin-dependent scattering off impurities in the bulk and/or at interfaces between the magnetic slabs and the spacer (extrinsic defects). It should be noted that in real multilayers also dislocations or stacking faults occur, and magnons and phonons can cause dynamical perturbations. A real multilayer system usually represents a mixture of both intrinsic and extrinsic defects.

Ab initio calculations of the GMR are still rather rare. We mention a Boltzmann-type approach developed for multilayer systems within the relaxation-time approximation,[7] which is limited to either weak scattering or very low concentration limits. Typically, the electronic structure of a three-dimensional periodic (infinite) multilayer system is determined, in particular the velocities at the Fermi surface. Then, in separate calculations, the spin-dependent relaxation time of bulk impurities is found and used to solve the (classical) Boltzmann equation. Clearly, the change of the superlattice band structure due to impurities is neglected, hence the above-mentioned limitations of the method. A solution of the Boltzmann equation for layered systems without the relaxation-time approximation has also been suggested.[8] Recently, *ab initio* calculations using a Kubo-Greenwood approach generalized to layered systems[9,10] and applied to the CIP geometry have appeared. In here (substitutional) disorder is included within an inhomogeneous coherent potential approximation (CPA). This is an appropriate approach to deal with the influence of imperfections and to treat intrinsic and extrinsic scattering on equal footing. However, up to now in there the so-called vertex corrections with respect to the configurational average of the products of two single particle Green's functions are neglected, an approximation that seems to be more justified for the CIP geometry than for the CPP geometry. In principle, however, the above-mentioned approaches can be used for both the CIP and CPP geometry.

An alternative theoretical approach based on nonequilibrium Green's functions or on a transmission matrix formalism (Landauer-type approach) can be used for the CPP transport. A useful review of these techniques based on the evaluation of the transmission matrix can be found in a recent monograph.[11]

It is the aim of this paper to formulate a surface Green's function (SGF) approach to CPP transport in magnetic mul-

tilayers within the tight-binding linear muffin-tin orbital (TB-LMTO) method[12] and to extend it to the case of lateral two-dimensional supercells with random occupation of lattice sites by two kinds of atoms. Our description thus allows us to treat specular and diffusive scattering on equal footing and on quantitative level, which is impossible in model calculations. This concerns, in particular, a detailed quantitative description of the electronic structure of the active part of the sample as well as of its leads. The usefulness of such an approach was recently illustrated for single-band[13,14] and two-band[15] TB models while empirical multiband tight-binding (TB) models were limited to specular scatterings only.[15–19] We therefore present a systematic study of the combined effect of specular and diffusive scatterings in various part of the system, namely of substitutional alloying in the spacer, in the magnetic slabs, and at their interfaces. The applications discussed refer to Co/Cu/Co(001)-based trilayers. An important part of this study is also the development of a formal theory of the Landauer-Büttiker-type approach to layered system in the framework of the TB-LMTO method. The computational scheme developed scales linearly with the number of principal layers and its efficiency is further increased by evaluating the lead supercell SGF from the SGF of the original two-dimensional lattice by means of a lattice Fourier transformation. This makes it possible to apply the supercell approach on *ab initio* level to relatively large random supercells.

II. FORMALISM

Suppose the magnetic multilayer system consists of nonrandom semi-infinite left ($\mathcal{L}$) and right ($\mathcal{R}$) leads sandwiching a trilayer consisting of a left and a right magnetic slab of varying thickness separated by a nonmagnetic spacer of varying thickness. It should be noted that left and right leads and magnetic slabs can consist of different metals. A repetition consists of two bilayers each of them formed by nonmagnetic and magnetic layers such that a ferromagnetic and an antiferromagnetic configuration per repetition can be formed. A special case of a trilayer consists of nonrandom semi-infinite left and right magnetic leads sandwiching a nonmagnetic spacer.

In principle, atomic layers can be viewed in terms of $n_1\times n_2$ supercells ($n_1\times n_2$ two-dimensional complex lattice). In order to describe disorder (substitutional binary alloys) it is then necessary to average over different occupations of the sites within the supercell by the two constituents involved and, at the end, to check the dependence of conductances on the supercell size. The stacking of such random layers in the growth direction can be arbitrary. Quite clearly such an approach applies to disordered spacers and/or magnetic slabs as well as to disordered interfaces.

In the following we neglect possible layer and lattice relaxations in the system; all formulations are based on an infinite parent lattice.[20]

A. Electronic structure

Within a nonrelativistic approach the electronic structure of the system is described in terms of the following (orthogonal) TB-LMTO Hamiltonian:

$$H^{\gamma,\sigma}_{\mathbf{R}L,\mathbf{R}'L'}=C^{\sigma}_{\mathbf{R}L}\delta_{\mathbf{R},\mathbf{R}'}\delta_{L,L'} +(\Delta^{\sigma}_{\mathbf{R}L})^{1/2}\{S^{\beta}[1-(\gamma^{\sigma}-\beta)S^{\beta}]^{-1}\}_{\mathbf{R}L,\mathbf{R}'L'} \times(\Delta^{\sigma}_{\mathbf{R}'L'})^{1/2}, \tag{1}$$

where $\mathbf{R}$ is the site index, σ is the spin index ($\sigma=\uparrow,\downarrow$), and the potential parameters $C^{\sigma}_{\mathbf{R}L}$, $\Delta^{\sigma}_{\mathbf{R}L}$, and $\gamma^{\sigma}_{\mathbf{R}L}$ are diagonal matrices with respect to the angular momentum $L=(\ell m)$. The nonrandom screened structure constants matrix $S^{\beta}_{\mathbf{R}L,\mathbf{R}'L'}$ and the site-diagonal screening matrix $\beta_{\mathbf{R},LL'}=\beta_L\,\delta_{L,L'}$ are spin independent. Assuming one and the same two-dimensional translational symmetry in each atomic layer p, $\mathbf{k}_{\parallel}$ projections can be defined, where $\mathbf{k}_{\parallel}$ is a vector from the corresponding surface Brillouin zone (SBZ). In a principal layer formalism,[12] the screened structure constants $S^{\beta}_{p,q}$ are of block tridiagonal form. Neglecting layer relaxations they are given by

$$S^{\beta}_{p,q}(\mathbf{k}_{\parallel})=\begin{cases} S^{\beta}_{0,0}(\mathbf{k}_{\parallel}); & q=p \\ S^{\beta}_{0,1}(\mathbf{k}_{\parallel}); & q=p+1 \\ S^{\beta}_{1,0}(\mathbf{k}_{\parallel}); & q=p-1 \\ 0; & \text{otherwise.} \end{cases} \tag{2}$$

The properties of individual atoms occupying lattice sites are characterized by screened potential function matrices:

$$P^{\beta,\sigma}_{\mathbf{R}L}(z)=\frac{z-C^{\sigma}_{\mathbf{R}L}}{\Delta^{\sigma}_{\mathbf{R}L}+(\gamma^{\sigma}_{\mathbf{R}L}-\beta_L)\,(z-C^{\sigma}_{\mathbf{R}L})}, \tag{3}$$

which are diagonal with respect to L. The potential functions assume the same value $P^{\beta,\sigma}_{p}(z)$ for each site within a given atomic layer p for 1×1 supercells, and, in principle, $n_1\times n_2$ different values $P^{\beta,\sigma}_{p,i}(z)$ for $n_1\times n_2$ supercells.

B. Surface Green's function

Within the TB-LMTO approach the Green's function (GF) matrix G^{σ} is given in terms of the auxiliary GF matrix $g^{\beta,\sigma}$ [12]

$$g^{\beta,\sigma}(\mathbf{k}_{\parallel},z)=[P^{\beta,\sigma}(z)-S^{\beta}(\mathbf{k}_{\parallel})]^{-1}, \tag{4}$$

namely as an infinite matrix with respect to the layer indices p,q. Assuming that the active part of the multilayer system consists of N layers and that the physical properties of all lead layers are identical, so-called embedding potentials $\Gamma^{\beta,\sigma}_{p}$[12] can be defined, which for $p=1$ and $p=N$ are given by

$$\Gamma^{\beta,\sigma}_{p}(\mathbf{k}_{\parallel},z)=\begin{cases} S^{\beta}_{1,0}(\mathbf{k}_{\parallel})\mathcal{G}^{\beta,\sigma}_{\mathcal{L}}(\mathbf{k}_{\parallel},z)S^{\beta}_{0,1}(\mathbf{k}_{\parallel}); & p=1 \\ S^{\beta}_{0,1}(\mathbf{k}_{\parallel})\mathcal{G}^{\beta,\sigma}_{\mathcal{R}}(\mathbf{k}_{\parallel},z)S^{\beta}_{1,0}(\mathbf{k}_{\parallel}); & p=N \\ 0; & \text{otherwise,} \end{cases} \tag{5}$$

where $\mathcal{G}^{\beta,\sigma}_{\mathcal{X}}$, $\mathcal{X}=\mathcal{L},\mathcal{R}$, are the corresponding surface Green's functions (SGF's) of the ideal left and right leads.

The layer-diagonal blocks of the inverse of the auxiliary Green's function matrix can then be written as

$$[g^{\beta,\sigma}(\mathbf{k}_\parallel,z)]^{-1}_{p,p} = \begin{cases} P_1^\beta(z) - S_{0,0}^{\beta,\sigma}(\mathbf{k}_\parallel) - \Gamma_1^{\beta,\sigma}(\mathbf{k}_\parallel,z); & p=1 \\ P_p^\beta(z) - S_{0,0}^{\beta,\sigma}(\mathbf{k}_\parallel); & 1<p<N \\ P_N^\beta(z) - S_{0,0}^{\beta,\sigma}(\mathbf{k}_\parallel) - \Gamma_N^{\beta,\sigma}(\mathbf{k}_\parallel,z); & p=N, \end{cases} \tag{6}$$

while its off-diagonal blocks ($1 \leqslant p,q \leqslant N$) are given by

$$[g^{\beta,\sigma}(\mathbf{k}_\parallel,z)]^{-1}_{p,q} = \begin{cases} -S_{0,1}^{\beta}(\mathbf{k}_\parallel); & q=p+1 \\ -S_{1,0}^{\beta}(\mathbf{k}_\parallel); & q=p-1 \\ 0; & \text{otherwise.} \end{cases} \tag{7}$$

It should be noted that Eqs. (5)–(7) only apply in the case of an infinite parent lattice (no layer relaxations). In this way the originally infinite matrix can easily be reduced to a finite matrix with the embedding potentials acting as boundary conditions. The block-tridiagonal form in Eq. (7) of the inverse of the Green's function allows to use efficient methods[12,21] to determine any nonvanishing block of $g_{p,q}^{\beta,\sigma}(\mathbf{k}_\parallel,z)$. In particular, this applies to the blocks $g_{1,N}^{\beta,\sigma}(z)$, $g_{N,1}^{\beta,\sigma}(z)$, and/or $g_{N,N}^{\beta,\sigma}(z)$ which are needed to evaluate the GMR described in the next subsection. For further details concerning the TB-LMTO method for layered systems we refer the reader to a recent book.[12]

In the case of two-dimensional $n_1 \times n_2$ (lateral) supercells the above expressions remain formally the same, however, each quantity has to be replaced by a supermatrix labeled by the positions of the sites within a given supercell. In the case of binary substitutional alloys the corresponding potential functions are assumed to have only two different values for the two constituents involved, i.e., we neglect possible local environment effects and short-range order within a given supercell. It should be noted, however, that in principle for each chosen supercell all inequivalent potential functions ought to be determined self-consistently (see also Sec. III A).

C. Magnetotransport

As is shown in the Appendix, the conductance per interface atom can be expressed as

$$\mathcal{C}_M = \sum_\sigma \mathcal{C}_M^\sigma, \quad \mathcal{C}_M^\sigma = \frac{e^2}{h}\frac{1}{N_\parallel}\sum_{\mathbf{k}_\parallel} T_M^\sigma(\mathbf{k}_\parallel,E_\mathrm{F}), \tag{8}$$

where $N_\parallel$ is the number of $\mathbf{k}_\parallel$ points in the SBZ, E_F is the Fermi energy, e is the electron charge, h is the Planck constant (the quantity $2e^2/h$ is usually called the conductance quantum), and $M=$FM (AF) denotes the ferromagnetic (antiferromagnetic) configuration of the magnetizations in the magnetic slabs. Furthermore, the transmission coefficients $T^\sigma(\mathbf{k}_\parallel,E)$ can be replaced by

$$\begin{aligned} T^\sigma(\mathbf{k}_\parallel,E) = \lim_{\delta\to 0+} \frac{1}{2}\mathrm{tr}\{ & B_1^{\beta,\sigma}(\mathbf{k}_\parallel,E) g_{1,N}^{\beta,\sigma}(\mathbf{k}_\parallel,z_+) \\ & \times B_N^{\beta,\sigma}(\mathbf{k}_\parallel,E) g_{N,1}^{\beta,\sigma}(\mathbf{k}_\parallel,z_-) + B_1^{\beta,\sigma}(\mathbf{k}_\parallel,E) \\ & \times g_{1,N}^{\beta,\sigma}(\mathbf{k}_\parallel,z_-) B_N^{\beta,\sigma}(\mathbf{k}_\parallel,E) g_{N,1}^{\beta,\sigma}(\mathbf{k}_\parallel,z_+)\}, \end{aligned} \tag{9}$$

where tr denotes the trace over angular momenta and sites per unit cell in a principal layer,

$$\begin{aligned} B_1^\sigma(\mathbf{k}_\parallel,E) &= i[\Gamma_1^{\beta,\sigma}(\mathbf{k}_\parallel,z_+) - \Gamma_1^{\beta,\sigma}(\mathbf{k}_\parallel,z_-)], \\ B_N^\sigma(\mathbf{k}_\parallel,E) &= i[\Gamma_N^{\beta,\sigma}(\mathbf{k}_\parallel,z_+) - \Gamma_N^{\beta,\sigma}(\mathbf{k}_\parallel,z_-)], \end{aligned} \tag{10}$$

and $z_\pm = E \pm i\delta$. In this formulation we have assumed a collinear spin structure, a generalization to noncollinear cases is given in Sec. II D. The magnetoresistance ratio is then defined as

$$\begin{aligned} GMR - \mathcal{R}_\mathrm{AF}/\mathcal{R}_\mathrm{FM} - 1 &= \mathcal{C}_\mathrm{FM}/\mathcal{C}_\mathrm{AF} - 1\,, \\ \mathcal{C}_\mathrm{M} &= \mathcal{C}_\mathrm{M}^\uparrow + \mathcal{C}_\mathrm{M}^\downarrow, \end{aligned} \tag{11}$$

where $\mathcal{R}_\mathrm{M} = 1/\mathcal{C}_\mathrm{M}$ is the resistance per interface atom.

It should be noted that the total transmittance is the sum of the transmission coefficients corresponding to all channels associated with a particular $\mathbf{k}_\parallel$. Therefore it may in general be a number larger than 1. The total number of channels (propagating and evanescent) is equal to the dimension of the matrices that enter Eq. (9). The number of propagating channels is $\mathbf{k}_\parallel$ dependent. Similarly, the total reflectance may in general be a number larger than 1 because the evanescent modes, which do not contribute to transport, formally appear here as channels with a reflection coefficient equal to 1.

In the (supercell) ballistic transport the choice of layers 1 and N in Eq. (9) is arbitrary. Consequently, one can identify them by viewing the left (semi-infinite) system to consist of the left lead and $N-1$ layers in the active part of the system, i.e., by using a different partitioning of the inverse of the Green's function matrix in Eq. (6) (see the Appendix). This formulation gives identical results but has computational advantages and was therefore employed in numerical studies in the next section.

Until now we have assumed simple systems with one atom at $\mathbf{t}_0$ in the two-dimensional elementary cell with translation vectors $\mathbf{a}_1$ and $\mathbf{a}_2$. The corresponding basis vectors of the two-dimensional reciprocal space are $\mathbf{b}_1$ and $\mathbf{b}_2$. Multilayers with disorder in the active region can be represented by finite supercells each containing n nonequivalent lattice sites occupied randomly by various atomic species. Let us assume that the supercell translation vectors are $\mathbf{A}_1 = n_1\mathbf{a}_1$ and $\mathbf{A}_2 = n_2\mathbf{a}_2$ ($n_1 \times n_2$ supercell, $n = n_1 n_2$). The basis vectors of the supercell reciprocal space are $\mathbf{B}_1 = \mathbf{b}_1/n_1$ and $\mathbf{B}_2 = \mathbf{b}_2/n_2$. The positions of atoms in the supercell are $\mathbf{t}_i = i_1\mathbf{a}_1 + i_2\mathbf{a}_2 + \mathbf{t}_0$, where $i=(i_1,i_2)$, $0 \leqslant i_i \leqslant n_i - 1$. The reciprocal-lattice vectors $\mathbf{Q}_j = j_1\mathbf{B}_1 + j_2\mathbf{B}_2$, where $j = (j_1,j_2)$, map the original SBZ onto the supercell SBZ (SCSBZ) in the sense that for each $\mathbf{k}_\parallel \in$ SBZ there exist just one $\mathbf{q}_\parallel \in$ SCSBZ and just one $\mathbf{Q}_j$ ($0 \leqslant j_i \leqslant n_i - 1$) such that $\mathbf{k}_\parallel = \mathbf{q}_\parallel + \mathbf{Q}_j$.

A generalization to supercells is easily achieved by substituting corresponding matrices by supermatrices labeled by individual atoms within a supercell. One can express the supercell (SC) SGF therefore in terms of the SGF of the original lattice as follows:

$$\mathcal{G}_{i,i'}^{sc}(\mathbf{q}_\parallel,z) = \frac{1}{n}\sum_{j=1}^{n} e^{-i\mathbf{Q}_j(\mathbf{t}_i - \mathbf{t}_{i'})}\mathcal{G}(\mathbf{q}_\parallel + \mathbf{Q}_j, z), \tag{12}$$

which significantly improves the efficiency of calculations.

D. Generalization to the noncollinear case

Magnetotransport in systems with noncollinearly aligned magnetizations of the magnetic slabs, e.g., the domain-wall magnetoresistance, requires to view the potential functions and the screened structure constants as 2×2 supermatrices in spin space. A rotation of the spin orientation in one particular layer p by an angle θ_p is then assumed to be with respect to the spin orientation of the topmost right magnetic layer of the active part of the system ($\theta=0$). Quite clearly, all translationally invariant atoms in a given plane of atoms have to have the same spin orientation.[20] The potential function in the local (rotated) coordinate system is block diagonal in spin space,

$$P_p^{\beta}(z)=\begin{pmatrix} P_p^{\beta,\uparrow}(z) & 0 \\ 0 & P_p^{\beta,\downarrow}(z) \end{pmatrix}. \tag{13}$$

It can be expressed in the global coordinate system by the following similarity transformation

$$P_p^{\beta}(z,\theta_p)=\mathrm{U}(\theta_p)P_p^{\beta}(z)\mathrm{U}^{\dagger}(\theta_p) \tag{14}$$

using the unitary rotation matrices $\mathrm{U}(\theta)$,

$$\mathrm{U}(\theta)=\begin{pmatrix} c & s \\ -s & c \end{pmatrix}, \tag{15}$$

where $c=\cos(\theta/2)$, $s=\sin(\theta/2)$. The structure constants in the global coordinate system are block diagonal,

$$S_{pq}^{\beta}(\mathbf{k}_{\parallel})=\begin{pmatrix} S_{pq}^{\beta,\uparrow}(\mathbf{k}_{\parallel}) & 0 \\ 0 & S_{pq}^{\beta,\downarrow}(\mathbf{k}_{\parallel}) \end{pmatrix}, \tag{16}$$

and $S_{pq}^{\beta,\uparrow}(\mathbf{k}_{\parallel})=S_{pq}^{\beta,\downarrow}(\mathbf{k}_{\parallel})$. The corresponding Green's function can be now obtained using Eqs. (14) and (16).

III. RESULTS AND DISCUSSION

We have performed calculations for the following multilayer system:

$$\begin{array}{c|c|c|c|c} \mathrm{Cu}(001) & M_m & S_s & M_m & \mathrm{Cu}(001) \\ \text{semi-infinite} & \text{magnetic} & \text{spacer} & \text{magnetic} & \text{semi-infinite}, \\ \text{left lead} & \text{slab} & & \text{slab} & \text{right lead} \end{array} \tag{17}$$

where the number of atomic layers in the active part of the system is $N=2m+s$, and all calculations are based on a fcc Co(001) parent lattice.

For $\mathrm{Co}_m/\mathrm{Cu}_s/\mathrm{Co}_m$ trilayers we have studied in the ballistic limit the dependence of the GMR on the thickness of the magnetic slabs m and the oscillatory behavior of the GMR with respect to the spacer thickness s. We then studied the effect of repeating a magnetic multilayer system by considering the case of $\mathrm{Cu}(001)/\mathrm{Co}_5\mathrm{Cu}_5\mathrm{Co}_5(\mathrm{Cu}_5\mathrm{Co}_5)_r/\mathrm{Cu}(001)$, which for $r=0$ reduces to a simple trilayer. As an example for noncollinear arrangements, we assumed a model for transport through a domain wall by considering the system $\mathrm{Co}(001)/\mathrm{Co}_D/\mathrm{Co}(001)$ with $\theta_L=0$, $\theta_R=\pi$, and $\theta_n=(\pi n)/D$, where θ_L, θ_R, and θ_n refer to the angles in Eq. (15) for the left semi-infinite system, the right semi-infinite system, and the nth layer in the active part of the system, respectively, and D denotes the thickness of the domain wall in monolayers (ML's).

The combined effect of intrinsic and extrinsic defects will be demonstrated for Co/Cu/Co-based trilayers, namely for: (i) interdiffused interfaces; (ii) a random spacer sandwiched by ideal magnetic slabs, and (iii) an ideal Cu spacer sandwiched by alloyed magnetic slabs.

A. Numerical implementation

Layer-wise substitutional alloys $A_{1-x}B_x$ are simulated by randomly occupying a chosen (in-plane) supercell with A and B atoms, such that their ratio corresponds to the overall concentration x. The random configurations were generated using the RM48 random number generator[22] and the binary correlation function was evaluated to test the ''randomness'' of each generated configuration. We have used 5×5 and 7×7 supercells corresponding roughly to a $A_{85}B_{15}$ random substitutional alloy, namely, 21 A atoms and 4 B atoms for the 5×5 supercell, 41 A atoms and 8 B atoms for the 7×7 supercell. In all cases (typically an average over five configurations for a 5×5 supercell and an average over three configurations for a 7×7 supercell were calculated) the results for the partial currents agreed within 1–3 % with each other, the agreement being better for larger supercells.

In principle, one should use self-consistent potential parameters corresponding to each configuration chosen and each size of supercell assumed. However, since such an approach is numerically prohibitive we have used self-consistent CPA potential parameters determined for a given alloy composition[12] also in the present supercell calculations. It should be noted that the same parameters were employed for various random configurations and different supercell sizes. We have thus neglected all possible fluctuations of the potential parameters due to a variation of the local environment and assumed that the potential parameters take only two values, namely the same for any A and B atom within a supercell. For cases of a 2×2 supercell (simulating $A_{75}B_{25}$ alloys) and a 3×3 supercell (simulating $A_{89}B_{11}$ alloys) we found that the fluctuations of the calculated potential parameters for A and B atoms for different random configurations from those obtained self-consistently using the CPA are quite small (of the order of a few percent). The potential parameters were determined self-consistently for each type of interface occurring in the system. Furthermore, we have neglected the weak layer dependence of the potential parameters close to the interface and used their bulklike values.

The $\mathbf{k}_{\parallel}$ integration covers 10 000 points in the full fcc (001) SBZ (400 or 196 points in the corresponding 5×5 or 7×7 supercell SBZ). In some cases, e.g., for the study of the oscillatory behavior of the GMR as a function of the spacer thickness, a much higher number of $\mathbf{k}_{\parallel}$ points was used to obtain well converged results. In all cases we have employed $|\mathrm{Im}\, z_{\pm}|=10^{-7}$ Ry. It should be noted that for a 1×1 supercell one can integrate over the irreducible part of the SBZ while for random supercells the $\mathbf{k}_{\parallel}$ integration has to be extended to the full supercell SBZ.

B. Ballistic transport

We shall start our discussion by a remark concerning some general features of the electronic structure of Cu bands and of Co spin-up (↑) and Co spin-down (↓) bands at the Fermi energy of Cu leads. It should be noted that by ''bands'' we mean the bands of the three-dimensional periodic bulk systems fcc Cu and fcc Co. Since the Cu and the Co↑ bands are very similar, they introduce only a very weak intrinsic scattering at the Cu/Co interface. Consequently, the transmission of ↑ electrons for a ferromagnetic alignment of the magnetizations [and hence also the corresponding conductance, see Eq. (9)] through the Co/Cu interfaces is large. As the large difference between the Cu and Co↓ bands can be viewed as an effective potential barrier at the interface for ↓ electrons, this in turn gives rise to much smaller FM↓ and AF conductances. It should be noted that in here we study only symmetrical trilayers implying identical values for the spin-up and spin-down conductances in the AF configuration. Finally, partial conductances in the ballistic regime, namely spin-up and spin-down conductances for the FM and AF configurations are independent of the sample thickness, with exception of possible quantum-size oscillations (see below).

1. Dependence on the thickness of magnetic slabs

The dependence of the GMR of ideal $Co_m/Cu_5/Co_m$ trilayers on the thickness of the magnetic slabs m is presented in Fig. 1. The most remarkable feature is a strong suppression of the GMR [Fig. 1(a)] for small thicknesses and a saturation at about 100% at large thicknesses. As can be seen from the partial conductances shown in Fig. 1(b) the oscillatory behavior of the magnetoresistance in Fig. 1(a) is caused by the oscillatory behavior of the FM↓ and AF conductances. Similar oscillations are also seen in the simpler case of a single Co slab of varying thickness embedded into the Cu host [empty symbols in Fig. 1(b)]. It should be noted that the GMR of finite Co slabs never reaches the limit of semi-infinite Co slabs since the ballistic conductances of Cu leads in the case of finite Co slabs are different from those of Co leads in the case of semi-infinite Co leads. The mentioned suppression of the GMR is quite likely due to an effective potential barrier in the $d\downarrow$ channel because of the above-mentioned large difference between the Cu- and Co↓ bands: a narrower magnetic slab allows for a larger transmission of electrons in the FM↓ and both AF channels. Consequently, the total AF conductance increases faster than the total FM conductance and hence the GMR ratio drops (see also Ref. 19).

2. Dependence on the thickness of the spacer

The effect of quantum current oscillations was studied by Mathon[17] using an empirical multiband TB model within a Kubo-Landauer-type approach by considering the dependence of the GMR on the thickness of the spacer. In Fig. 2 we present such a study for $Co_5/Cu_s/Co_5$ trilayers with varying spacer thickness s. We clearly observe pronounced GMR oscillations [Fig. 2(a)] around a value of about 115% which are damped with increasing spacer thickness. A clearer picture is obtained by looking at the partial conductances. From Fig. 2(b) it can be seen that the oscillatory behavior originates mostly from the FM↓ conductance whose amplitudes are much larger than those of the AF conductance, while the FM↑ conductance is essentially thickness independent. We observe oscillations with a period of about 5–6 ML's for the FM↓ and AF conductance and, in addition, some admixture of short-period oscillations with a period of about 2.5 ML's is seen for the FM↓ conductance. These periods correlate reasonably well with similar values obtained for the interlayer exchange coupling using the same electronic structure model (see, e.g., Ref. 23). The amplitudes are roughly damped as s^{-1}, where s is the spacer thickness.[17]

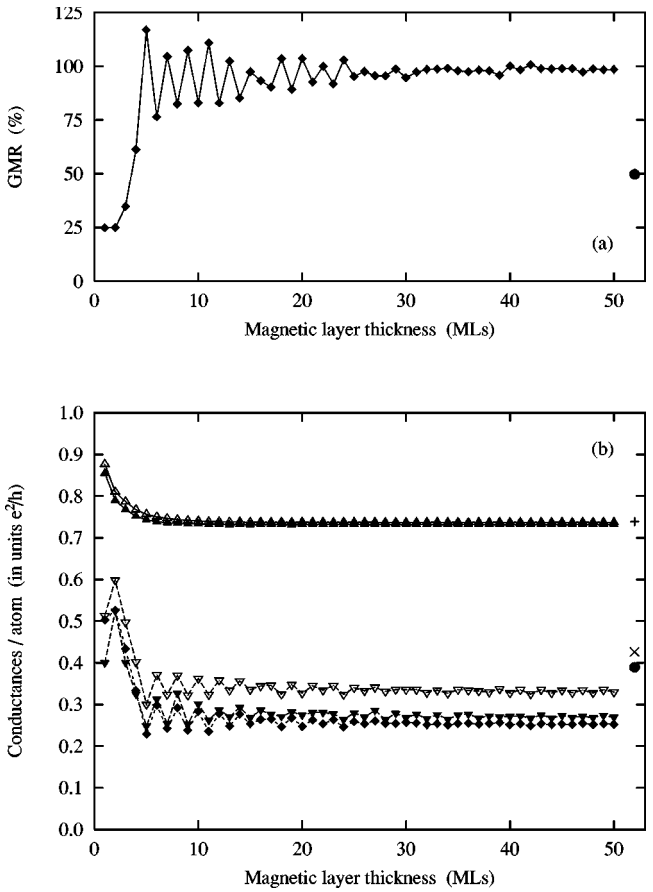

FIG. 1. Ideal $Co_m/Cu_5/Co_m$ trilayers sandwiched by semi-infinite Cu leads with varying thickness m of the magnetic slabs: (a) magnetoresistance ratio (diamonds) and the limit of semi-infinite Co slabs (bullet); (b) conductances per atom for the ferromagnetic ↑ spin (up triangles), ferromagnetic ↓ spin (down triangles), and antiferromagnetic configuration (diamonds). Empty symbols (up and down triangles) refer to the ferromagnetic ↑ and ↓ spin conductances of a single Co slab of varying thickness embedded into a Cu host. For semi-infinite Co slabs the ferromagnetic ↑ (+), ↓ (×), and antiferromagnetic (bullet) conductances are shown, respectively.

3. Co/Cu multilayers

GMR measurements are usually performed for two different kinds of systems, namely (i) spin valves modeled in the present paper by a trilayer and (ii) repeated multilayers. Such a repeated multilayer is modeled in here by adding a finite number of repetitions $Cu_5Co_5Cu_5Co_5$ to the reference trilayer $Co_5Cu_5Co_5$ (either from the left or from the right) and then

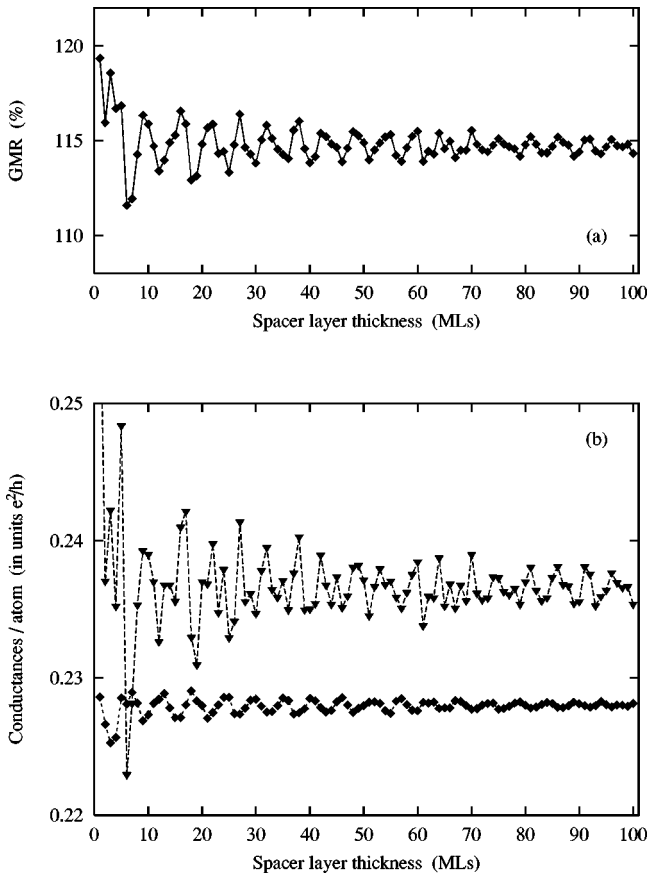

FIG. 2. Ideal $Co_5/Cu_s/Co_5$ trilayers sandwiched by semi-infinite Cu leads with varying spacer thickness *s*: (a) magnetoresistance ratio (diamonds); (b) conductances per atom for the ferromagnetic ↓ spin (down triangles) and antiferromagnetic configuration (diamonds). Note the reduced scale on the vertical axis compared to Fig. 1.

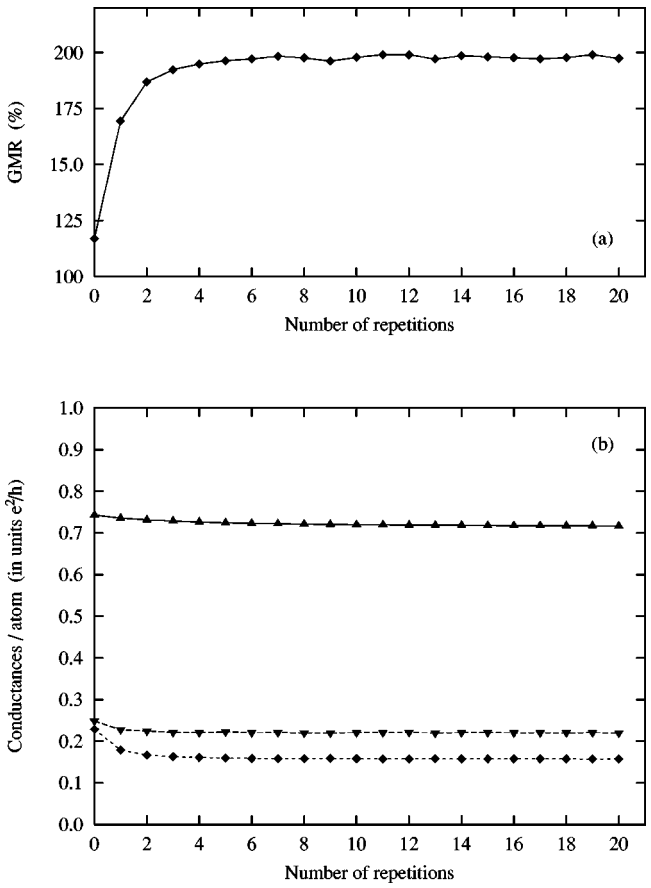

FIG. 3. Co/Cu multilayer treated as an ideal trilayer $Co_5/Cu_5/Co_5(Cu_5Co_5Cu_5Co_5)_r$ with r repetitions of the type $(Cu_5Co_5Cu_5Co_5)$ and sandwiched by semi-infinite Cu leads: (a) magnetoresistance ratio (diamonds); (b) conductances per atom for the ferromagnetic ↑ spin (up triangles), ferromagnetic ↓ spin (down triangles), and antiferromagnetic configuration (diamonds). The values for $r=0$ correspond to the trilayer $Co_5/Cu_5/Co_5$.

sandwiching the system by semi-infinite Cu leads. The chosen spacer thickness of 5 Cu ML's corresponds to the AF exchange coupling regime in the trilayer $Co_5Cu_5Co_5$ (see Ref. 23 for an evaluation of the interlayer exchange coupling within the present model). Figure 3 shows the GMR as a function of the number of repetitions r (each repetition amounts to 20 atomic layers) whereby $r=0$ corresponds to the reference trilayer. We observe a rather rapid formation of a saturation value (approximately twice as big as the value for a trilayer) within about five repetitions, the oscillations about the saturation value being very small. These features are in a good agreement with those in Ref. 24. In particular, it is obvious from Fig. 3(b) that the increase of the GMR with the number of repetitions can be related to a corresponding decrease in the AF conductance.

4. Domain-wall magnetoresistance

The problem of a domain-wall magnetoresistance (DWMR) was addressed recently using model[25,26] as well as realistic[27] calculations. As an illustration for perpendicular electric transport in noncollinearly ordered structures in Fig. 4 a first study of the DWMR for domain walls of varying thickness is shown. In this model calculations we simply assume a linear variation of the layer-wise rotation angle $\theta_n=(\pi n)/D$ within a domain wall of the thickness D. As can be seen from this figure a large DWMR is only obtained for domain-wall thicknesses of atomic scale (so-called constrictions[26,28]) while for thicker domain walls the DWMR quickly drops to almost zero. By comparing these with the ferromagnetic conductance, it is obvious from Fig. 4(b) that the conductance is decreased by the presence of domain walls. Finally, we mention that the conductance varies as D^{-1}, i.e., the resistance varies approximately linearly with the domain-wall thickness. All these results are in agreement with the conclusions in Ref. 27. It should be noted, however, that further studies are needed, in particular including the effect of impurities,[25] but also considering more realistic variations of the layer-wise rotation angles θ_n.

C. Combined ballistic and diffusive transport

In real systems, in addition to specular scattering at intrinsic defects (system interfaces) there is scattering at extrinsic defects, namely at impurities, stacking faults, dislocations, and there are even dynamical effects like scattering of electrons with phonons or magnons. In here we consider only substitutional impurities in the spacer, magnetic slabs, and at their interfaces in a reference system which consists of left and right semi-infinite Cu leads sandwiching two Co slabs,

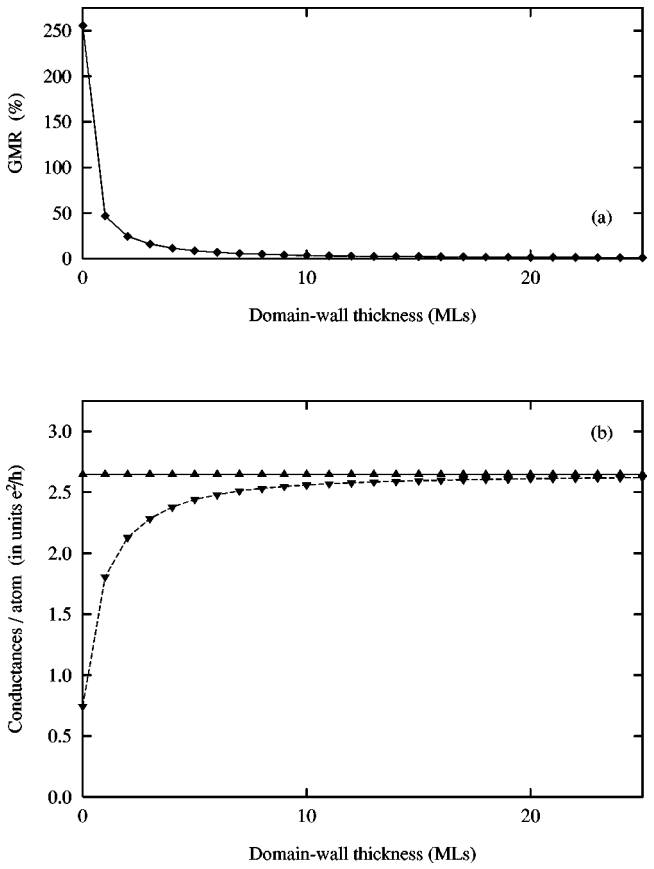

FIG. 4. A magnetic domain wall of varying thickness sandwiched by antiferromagnetically aligned semi-infinite Co leads. The layer-wise magnetization rotation angle varies linearly with the domain-wall thickness between 0 and π: (a) domain-wall magnetoresistance ratio; (b) total conductances per atom for the ferromagnetic configuration (up triangles), and for the domain wall (down triangles). Ferromagnetic configuration is infinite Co bulk.

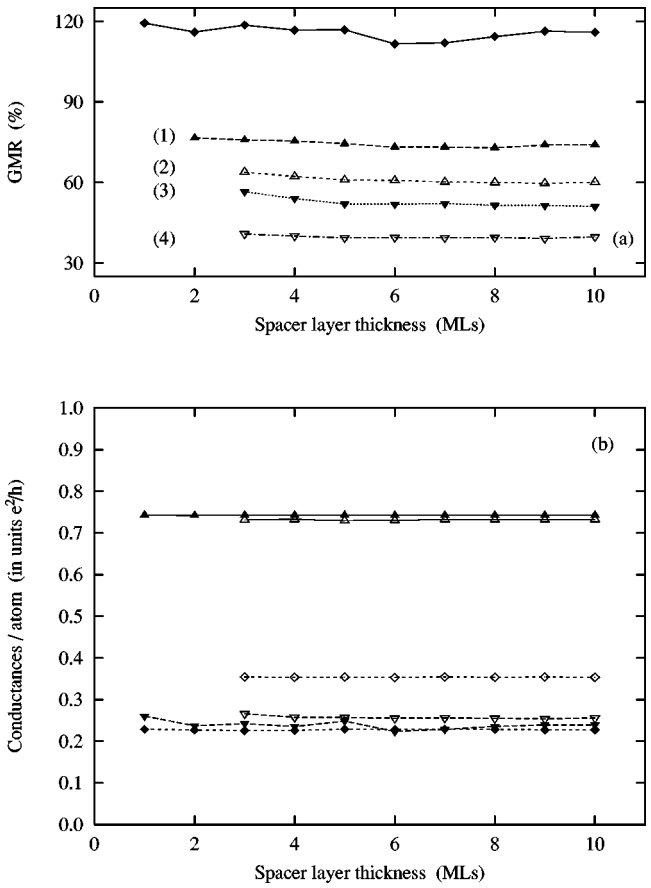

FIG. 5. Comparison of trilayers with 15%-interdiffused interfaces with ideal $Co_5/Cu_s/Co_5$ trilayers sandwiched by semi-infinite Cu leads as a function of the spacer thickness *s*: (a) magnetoresistance ratio (diamonds, ideal trilayer; up triangles (1), one of the inner interfaces is interdiffused; empty up triangles (2), both inner interfaces are interdiffused; down triangles (3), two inner and one of outer interfaces are interdiffused; empty down triangles (4), all four interfaces are interdiffused); (b) conductances per atom for the ferromagnetic ↑ spin (up triangles), ferromagnetic ↓ spin (down triangles), and antiferromagnetic configuration (diamonds). Full symbols refer to an ideal trilayer, empty symbols to a trilayer with all interfaces interdiffused.

each 5 ML's thick, and separated by a Cu spacer of varying thickness (1–10 ML's). In general, disorder can cause the following effects: (i) an increase of the overall amount of scattering which in turn contributes to a reduction of the transmission probability; (ii) a violation of the strict conservation of the $\mathbf{k}_\parallel$ vector belonging to the SBZ of leads can open new transmission channels which contribute to an increase of the conductance; (iii) interdiffusion smoothens the potential barrier in the ideal trilayer which in turn also leads to an increased transmission coefficient; and (iv) alloying in the magnetic layers can increase (decrease) the effective barrier for electrons at the Co/Cu interface and thus decrease (increase) the conductance in this channel. Therefore the net influence of disorder on the conductance results from a competition between all these effects and may lead to an increase or decrease of the conductance, depending on the system under consideration (see also Ref. 29).

1. Interface interdiffusion

The effect of disorder at the Co/Cu interfaces is shown in Fig. 5. The interdiffused interface extends over two neighboring layers of compositions $Co_{85}Cu_{15}$ (on the Co side) and $Co_{15}Cu_{85}$ (on the Cu side). As can be seen the GMR decreases monotonically with the number of disordered interfaces, and disorder suppresses the oscillations present for ideal interfaces. Disorder influences the FM↑ conductance very weakly because the Cu bands are similar in shape to the Co↑ bands. The AF conductance, however, is much larger than the one for the ideal trilayer and origins of this effect were discussed above [see points (ii) and (iii) at the beginning of Sec. III C]. Similar, but weaker effect, is observed also for FM↓ conductance. It could be concluded therefore that the decrease of the GMR is controlled by the increase of AF conductance due to the interface interdiffusion. It should be noted that partial conductances remain constant with the varying spacer thickness as the number of disordered layers does not change and possible quantum oscillations are damped by disorder.

2. Disorder in the spacer

The effect of alloying in the nonmagnetic spacer ($Cu_{85}Pd_{15}$ and $Cu_{50}Pd_{50}$) on the magnetoresistance is presented in Fig. 6. We observe a monotonic decrease of the

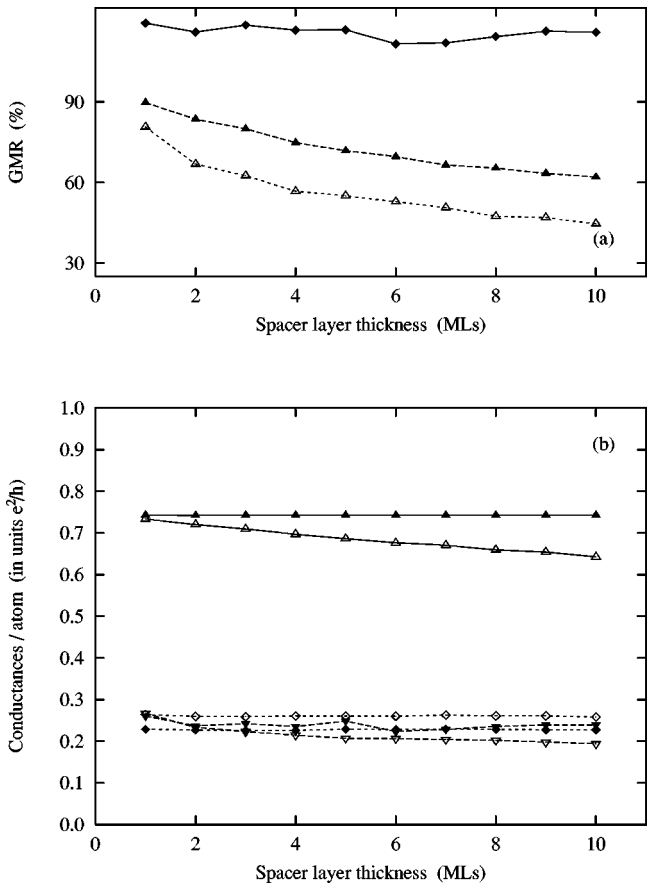

FIG. 6. Comparison of $Co_5/(Cu_{100-x}Pd_x)_s/Co_5$ trilayers ($x=15$ and 50) with ideal $Co_5/Cu_s/Co_5$ trilayers sandwiched by semi-infinite Cu leads as a function of the spacer thickness s: (a) magnetoresistance ratio (diamonds, ideal trilayer; full triangles, alloyed spacer with $x=15$; empty triangles, alloyed spacer with $x=50$); (b) conductances per atom for the ferromagnetic ↑ spin (up triangles), ferromagnetic ↓ spin (down triangles), and antiferromagnetic configuration (diamonds). Full symbols refer to an ideal trilayer, empty symbols to a trilayer with an alloyed spacer corresponding to $x=15$.

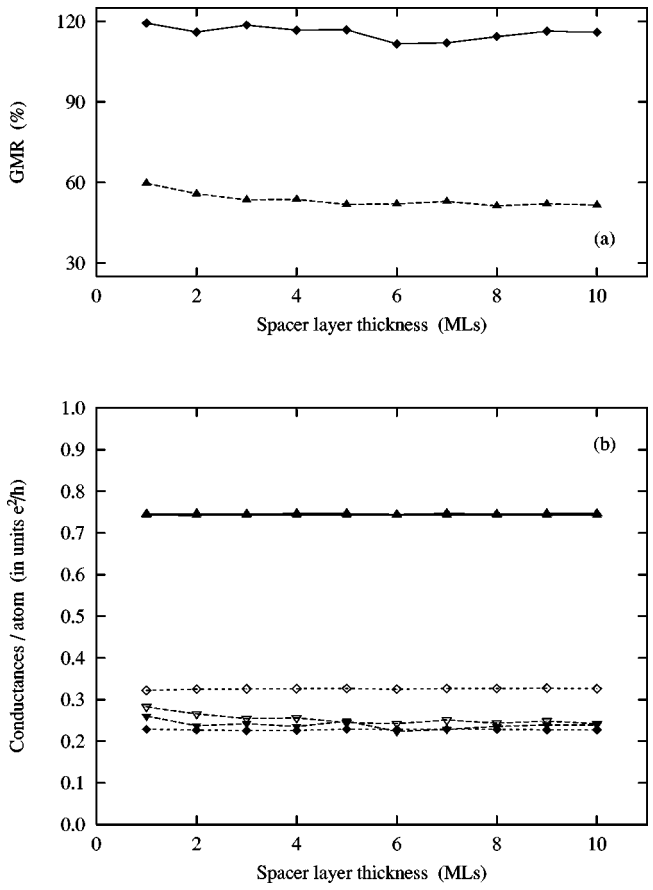

FIG. 7. Comparison of $(Co_{85}Ni_{15})_5/Cu_s/(Co_{85}Ni_{15})_5$ trilayers with ideal $Co_5/Cu_s/Co_5$ trilayers sandwiched by semi-infinite Cu leads as a function of the spacer thickness s: (a) magnetoresistance ratio (diamonds, ideal trilayer; triangles, alloyed magnetic slabs); (b) conductances per atom for the ferromagnetic ↑ spin (up triangles), ferromagnetic ↓ spin (down triangles), and antiferromagnetic configuration (diamonds). Full symbols refer to an ideal trilayer, empty symbols to a trilayer with alloyed magnetic layers.

GMR ratio as a function of the spacer thickness [Fig. 6(a)]. The origin of this decrease can be traced from Fig. 6(b). It should be noted that in Cu-rich alloys the states at the Fermi energy are influenced only weakly by impurities.[30] Therefore, the FM↓ and AF conductances are only slightly smaller than those of an ideal trilayer. Consequently, the effect of extrinsic potential scattering for the FM↓ and AF conductance is rather small as compared to the strong intrinsic scattering at the interfaces. On the other hand, the effect of extrinsic defects dominates the FM↑ conductance where intrinsic scattering is negligibly small. In fact it is the FM↑ channel which is mostly responsible for the decrease of the GMR ratio with increasing spacer thickness. Essentially linear decrease of the FM↑ conductance as a function of the spacer thickness indicates the ohmic transport regime in this case which is easy to understand as the number of disordered layers increases with the spacer thickness in contrast to the previous case of interface interdiffusion. The above conclusions remain qualitatively the same for a $Cu_{50}Pd_{50}$ case but the effect of disorder is larger as compared to a $Cu_{85}Pd_{15}$ spacer.

3. Disorder in magnetic layers

The effect of alloying in the magnetic slabs on the magnetoresistance is shown in Figs. 7 and 8. In these we have considered two different situations, namely $Co_{85}Ni_{15}$ and $Co_{85}Cr_{15}$ magnetic slabs. In the former case the local magnetic moments of Co and Ni are oriented parallel while the Co and Cr moments in $Co_{85}Cr_{15}$ are aligned antiparallel. Contrary to the case of disorder in the spacer in the $Co_{85}Ni_{15}$ case (Fig. 7) the GMR ratio quickly saturates at approximately half of the value for an ideal trilayer. The behavior of the partial conductances is similar to that for an interdiffused interface. Due to the similarity of the Co↑ and the Ni↑ bands at the Fermi energy the FM↑ conductance is nearly the same as for the ideal trilayer. Since the Co↓ bands are higher in energy as compared to the Ni↓ bands, alloying of Co with Ni decreases effectively the potential barrier height at the interface resulting thus in a larger transmission coefficient (conductance) as compared to the ideal trilayer. Consequently, the AF conductance of the alloyed magnetic layers is larger than for an ideal trilayer. The same effect, but much weaker, applies for the FM↓ conductance indicating dominating intrinsic scattering at interfaces for this channel. The behavior of $Co_{85}Cr_{15}$ magnetic slabs is quite different (see Fig. 8),

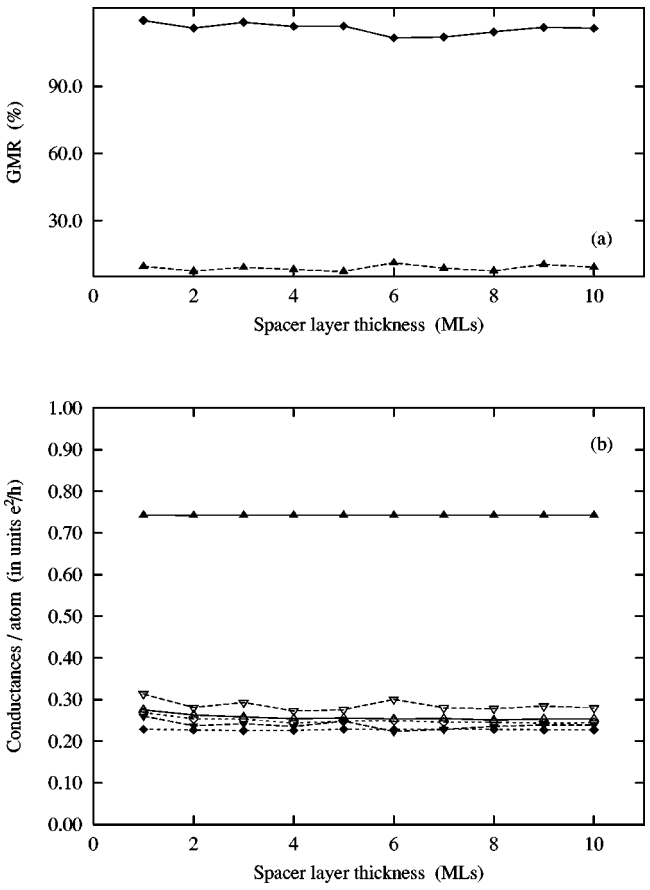

FIG. 8. Comparison of $(Co_{85}Cr_{15})_5/Cu_s/(Co_{85}Cr_{15})_5$ trilayers with ideal $Co_5/Cu_s/Co_5$ trilayers sandwiched by semi-infinite Cu leads as a function of the spacer thickness *s*: (a) magnetoresistance ratio (diamonds, ideal trilayer; triangles, alloyed magnetic slabs); (b) conductances per atom for the ferromagnetic ↑ spin (up triangles), ferromagnetic ↓ spin (down triangles), and antiferromagnetic configuration (diamonds). Full symbols refer to an ideal trilayer, empty symbols to a trilayer with alloyed magnetic layers.

because due to the antiparallel orientation of moments for Co and Cr sites, even the FM↑ conductance is influenced by disorder. In fact, in all channels the conductance is now approximately the same, causing the GMR ratio to be strongly suppressed.

IV. CONCLUSIONS

We have presented a systematic *ab initio* study of the influence of alloying in the spacer, magnetic layers, and at interfaces on the CPP transport in magnetic multilayers. The electronic structure is described by the TB-LMTO method while a Landauer-Büttiker-type approach formulated within the framework of surface Green's functions is used to evaluate transport properties. A generalization to noncollinear magnetic configurations, as would apply for a description of domain walls, was also studied.

We have considered a variety of magnetic multilayers based on the reference Co/Cu/Co(001) trilayer system which exhibit various kinds of transport ranging from the ballistic regime to the diffusive regime. The results of the numerical calculations were discussed in terms of partial conductances of the ↑ and ↓ channels in the FM and the AF alignment. In general, the GMR ratio decreases with introducing impurities in different parts of the sample while the partial conductances may both increase or decrease due to disorder in layered systems. The present results seem to be valid for quite a few magnetic multilayer systems since the scattering at the magnetic/nonmagnetic interface in one spin channel can significantly be larger than in the other channel (similarly as for the Co/Cu interface studied here). We also discussed the effect of quantum oscillations of the magnetocurrent and quasiperiodicity in repeated multilayers. Extensive numerical tests seem to indicate that already 5×5 supercells containing 25 atoms averaged over a limited number of random configurations (typically a configurational average over five different configurations was employed) give representative results for the CPP magnetoresistance. The present approach can also be generalized to the case of transport across a barrier of a different kind such as in semiconductor or transition-metal oxide tunneling junctions.

ACKNOWLEDGMENTS

Financial support for this work was provided by the Grant Agency of the Academy of Sciences of the Czech Republic (Project No. A1010829), the Grant Agency of the Czech Republic (Project No. 202/00/0122), the MSMT of the Czech Republic (COST P3.70), the Center for Computational Materials Science in Vienna (GZ 45.442 and GZ 45.420), the Austrian Science Foundation (FWF T27-TPH), the TMR Network ''Interface Magnetism'' (Contract No. EMRX-CT96-0089), and the RTN Network ''Computational Magnetoelectronics'' (Contract No. RTN1-1999-00145) of the European Commission.

APPENDIX: CONDUCTANCE

The orthogonal Hamiltonian given in Eq. (1) yields an accurate description of the electronic structure for most close-packed transition-metal systems but it is not short ranged. For a physically more transparent derivation of electric transport properties a less accurate (first-order) but short-ranged Hamiltonian,[12,31] defined as

$$H^{\beta,\sigma}_{\mathbf{R}L,\mathbf{R}'L'}=C^{\beta,\sigma}_{\mathbf{R}L}\delta_{\mathbf{R}\mathbf{R}'}\delta_{LL'}+(\Delta^{\beta,\sigma}_{\mathbf{R}L})^{1/2}S^{\beta}_{\mathbf{R}L,\mathbf{R}'L'}(\Delta^{\beta,\sigma}_{\mathbf{R}'L'})^{1/2}, \tag{A1}$$

represents a much better starting point. This Hamiltonian refers to the following approximation for the screened potential functions

$$\tilde{P}^{\beta,\sigma}_{\mathbf{R}L}(z)=\frac{z-C^{\beta,\sigma}_{\mathbf{R}L}}{\Delta^{\beta,\sigma}_{\mathbf{R}L}}, \tag{A2}$$

where at a particular energy E, namely, at the Fermi energy E_F of the system, the potential parameters $C^{\beta,\sigma}_{\mathbf{R}L}$ and $\Delta^{\beta,\sigma}_{\mathbf{R}L}$ have to fulfill the following conditions [cf. Eqs. (3) and (A2)]:

$$\tilde{P}^{\beta,\sigma}_{\mathbf{R}L}(E_F)=P^{\beta,\sigma}_{\mathbf{R}L}(E_F), \quad \left.\frac{d\tilde{P}^{\beta,\sigma}_{\mathbf{R}L}(z)}{dz}\right|_{z=E_F}=\left.\frac{dP^{\beta,\sigma}_{\mathbf{R}L}(z)}{dz}\right|_{z=E_F}. \tag{A3}$$

The matrix elements of the operator of the z coordinate can be approximated within the TB-LMTO formalism as

$$Z_{\mathbf{R}L,\mathbf{R}'L'}=\delta_{\mathbf{R}L,\mathbf{R}'L'}z_{\mathbf{R}}, \tag{A4}$$

where $z_{\mathbf{R}}$ denotes the z coordinate of the center of the $\mathbf{R}$th Wigner-Seitz sphere. This approximation was used in previous TB-LMTO studies of electron transport[32,33] and its more detailed discussion will be given elsewhere.[34]

The short-ranged Hamiltonian given in Eq. (A1) can be written as a sum over $\mathbf{k}_\parallel$ vectors. Let us consider the Hamilton operator of a quasi-one-dimensional system for a particular $\mathbf{k}_\parallel$ vector (variable $\mathbf{k}_\parallel$ is omitted here),

$$\hat{H}=\sum_p\,[\hat{H}_{p,p}+\hat{H}_{p,p+1}+\hat{H}_{p,p-1}], \tag{A5}$$

with interactions only between the neighboring principal layers p and whose blocks are given by $\hat{H}_{p,q}=\Pi_p\hat{H}_{p,q}\Pi_q=\Pi_p\hat{H}\Pi_q$, where Π_p is a projector onto the layer p.

The operator $\hat{Z}$ of the coordinate perpendicular to the atomic planes and the operator $\hat{v}$ of the corresponding velocity are then given by

$$\hat{Z}=d\sum_p\,p\Pi_p,\quad \hat{v}=\frac{1}{i\hbar}[\hat{Z},\hat{H}]=\frac{d}{i\hbar}\sum_p\,[\hat{H}_{p+1,p}-\hat{H}_{p,p+1}], \tag{A6}$$

where d is the interlayer distance.

The operator $\hat{J}$ of the electric current perpendicular to the atomic layers can then be written as a sum of currents $\hat{J}_{p,p+1}$ between layers p and $p+1$

$$\hat{J}=\frac{1}{M}\sum_p\,\hat{J}_{p,p+1},\quad \hat{J}_{p,p+1}=\frac{e}{i\hbar}[\hat{H}_{p+1,p}-\hat{H}_{p,p+1}], \tag{A7}$$

where M is the number of layers which, in principle, has to be taken to infinity. Note that the interlayer distance d disappears due to the normalization.

In the linear response regime the conductance for a particular channel $(\mathbf{k}_\parallel,\sigma)$ at an energy E can be expressed as

$$C(E)=\pi\hbar\sum_{\alpha,\beta}\,|\langle\alpha|\hat{J}|\beta\rangle|^2\,\delta(E-E_\alpha)\,\delta(E-E_\beta) \tag{A8}$$

$$=\frac{\pi\hbar}{M^2}\sum_{\alpha,\beta}\sum_{p,q}\,\langle\alpha|\hat{J}_{p,p+1}|\beta\rangle\langle\beta|\hat{J}_{q,q+1}|\alpha\rangle\,\delta(E-E_\alpha)\times\delta(E-E_\beta). \tag{A9}$$

In Eq. (A8) $|\alpha\rangle$ and $|\beta\rangle$ are (orthonormalized) eigenstates of the Hamiltonian $\hat{H}$, Eq. (A5). The double sum over the layer indices p and q in Eq. (A9) can be eliminated due to current conservation.[35] The layer indices p and q may then be chosen arbitrarily which yields

$$C(E)=\pi\hbar\sum_{\alpha,\beta}\,\langle\alpha|\hat{J}_{p,p+1}|\beta\rangle\langle\beta|\hat{J}_{q,q+1}|\alpha\rangle\times\delta(E-E_\alpha)\,\delta(E-E_\beta). \tag{A10}$$

The δ functions in Eq. (A10) can be expressed in terms of the resolvent $\hat{G}(z)=[z-\hat{H}]^{-1}$ of the Hamiltonian $\hat{H}$ as

$$\sum_\alpha\,|\alpha\rangle\,\delta(E-E_\alpha)\langle\alpha|=\frac{1}{2\pi i}[\hat{G}(E-i0)-\hat{G}(E+i0)], \tag{A11}$$

such that

$$C(E)=\frac{e^2}{2h}\mathrm{Tr}\{(\hat{H}_{p+1,p}-\hat{H}_{p,p+1})[\hat{G}(E-i0)-\hat{G}(E+i0)]\times(\hat{H}_{q+1,q}-\hat{H}_{q,q+1})[\hat{G}(E-i0)-\hat{G}(E+i0)]\}, \tag{A12}$$

where Tr denotes the trace over all lattice sites and angular momenta including the spin.

The total conductance per two-dimensional elementary cell is then given by the Kubo-Greenwood formula as

$$\mathcal{C}=\frac{e^2}{h}\sum_\sigma\,\frac{1}{N_\parallel}\sum_{\mathbf{k}_\parallel}\,\int\,dE[-f'(E)]T^\sigma(\mathbf{k}_\parallel,E), \tag{A13}$$

where $f(E)$ is the Fermi-Dirac function. At $T=0$ the integration is trivial and all the quantities need to be evaluated only at the Fermi energy E_F. The transmission probability $T^\sigma(\mathbf{k}_\parallel,E)$ for the channel $(\mathbf{k}_\parallel,\sigma)$ at energy E reduces therefore to

$$\begin{aligned}T^\sigma(\mathbf{k}_\parallel;E)=\frac{1}{2}\sum_{\mu,\nu}\,(-1)^{\mu+\nu}\,\mathrm{tr}\{&H^\sigma_{p,p+1}(\mathbf{k}_\parallel)G^\sigma_{p+1,q}(\mathbf{k}_\parallel,z_\mu)\\&\times H^\sigma_{q,q+1}(\mathbf{k}_\parallel)G^\sigma_{q+1,p}(\mathbf{k}_\parallel,z_\nu)+H^\sigma_{p+1,p}(\mathbf{k}_\parallel)\\&\times G^\sigma_{p,q+1}(\mathbf{k}_\parallel,z_\mu)H^\sigma_{q+1,q}(\mathbf{k}_\parallel)G^\sigma_{q,p+1}(\mathbf{k}_\parallel,z_\nu)\\&-H^\sigma_{p,p+1}(\mathbf{k}_\parallel)G^\sigma_{p+1,q+1}(\mathbf{k}_\parallel,z_\mu)H^\sigma_{q+1,q}(\mathbf{k}_\parallel)\\&\times G^\sigma_{q,p}(\mathbf{k}_\parallel,z_\nu)-H^\sigma_{p+1,p}(\mathbf{k}_\parallel)G^\sigma_{p,q}(\mathbf{k}_\parallel,z_\mu)\\&\times H^\sigma_{q,q+1}(\mathbf{k}_\parallel)G^\sigma_{q+1,p+1}(\mathbf{k}_\parallel,z_\nu)\}.\end{aligned} \tag{A14}$$

Here the indices $\mu,\nu=1,2$ are chosen such that $z_\mu=E+i\delta$ if $\mu=1$, $z_\mu=E-i\delta$ if $\mu=2$, where δ is a small positive constant, and similar relations apply for z_ν. All quantities in Eq. (A14) are matrices with respect to angular momentum indices L,L' and tr denotes the trace over angular momenta. At this stage, by setting $p=q=0$ one can directly retrieve the expression for conductance given by Mathon *et al.*[17]

Within the LMTO formalism by using Eqs. (4), (A1), and (A2), and omitting for matters of simplicity the variable $\mathbf{k}_\parallel$ and the superscript β, we obtain

$$\begin{aligned}T^\sigma(E)=\frac{1}{2}\sum_{\mu,\nu}\,(-1)^{\mu+\nu}\,\mathrm{tr}\{&S_{0,1}g^\sigma_{p+1,q}(z_\mu)S_{0,1}g^\sigma_{q+1,p}(z_\nu)\\&+S_{1,0}g^\sigma_{p,q+1}(z_\mu)S_{1,0}g^\sigma_{q,p+1}(z_\nu)\\&-S_{0,1}g^\sigma_{p+1,q+1}(z_\mu)S_{1,0}g^\sigma_{q,p}(z_\nu)\\&-S_{1,0}g^\sigma_{p,q}(z_\mu)S_{0,1}g^\sigma_{q+1,p+1}(z_\nu)\}.\end{aligned} \tag{A15}$$

This expression is a formal modification of Eq. (A14), namely the screened structure constants S and the auxiliary

Green's function $g(z)$ substitute the Hamiltonian H and its resolvent $G(z)$. It should be noted that the derivation of Eq. (A15) was based on the first-order Hamiltonian, Eq. (A1), but as can be shown[34] it is valid also for the orthogonal LMTO Hamiltonian, Eq. (1). Furthermore, the expression in Eq. (A15) is invariant with respect to the LMTO representation, i.e., one can use also the most localized representation β[12] for transport problems.

The expression in Eq. (A15) can further be simplified by using surface Green's functions of the left $[\mathcal{G}^{\sigma}_{\mathcal{L}}(z)]$ and right $[\mathcal{G}^{\sigma}_{\mathcal{R}}(z)]$ lead. We first set $p=0$, $q=N$ and insert the identities given below into Eq. (A15):

$$
\begin{aligned}
g^{\sigma}_{N+1,0}(z_\nu) &= \mathcal{G}^{\sigma}_{\mathcal{R}}(z_\nu) S_{1,0} g^{\sigma}_{N,1}(z_\nu) S_{1,0} \mathcal{G}^{\sigma}_{\mathcal{L}}(z_\nu),\\
g^{\sigma}_{0,N+1}(z_\mu) &= \mathcal{G}^{\sigma}_{\mathcal{L}}(z_\mu) S_{0,1} g^{\sigma}_{1,N}(z_\mu) S_{0,1} \mathcal{G}^{\sigma}_{\mathcal{R}}(z_\mu),\\
g^{\sigma}_{1,N+1}(z_\mu) &= g^{\sigma}_{1,N}(z_\mu) S_{0,1} \mathcal{G}^{\sigma}_{\mathcal{R}}(z_\mu),\\
g^{\sigma}_{N,0}(z_\nu) &= g^{\sigma}_{N,1}(z_\nu) S_{1,0} \mathcal{G}^{\sigma}_{\mathcal{L}}(z_\nu),\\
g^{\sigma}_{0,N}(z_\mu) &= \mathcal{G}^{\sigma}_{\mathcal{L}}(z_\mu) S_{0,1} g^{\sigma}_{1,N}(z_\mu),\\
g^{\sigma}_{N+1,1}(z_\nu) &= \mathcal{G}^{\sigma}_{\mathcal{R}}(z_\nu) S_{1,0} g^{\sigma}_{N,1}(z_\nu),
\end{aligned}
\tag{A16}
$$

which easily can be proved using the partitioning technique (see, e.g., Refs. 21 and 36). Thus we obtain

$$
\begin{aligned}
T^{\sigma}(E) = \frac{1}{2}\sum_{\mu,\nu} (-1)^{\mu+\nu} \mathrm{tr}\{ & S_{1,0} g^{\sigma}_{1,N}(z_\mu) S_{0,1} \mathcal{G}^{\sigma}_{\mathcal{R}}(z_\nu)\\
&\times S_{1,0} g^{\sigma}_{N,1}(z_\nu) S_{1,0} \mathcal{G}^{\sigma}_{\mathcal{L}}(z_\nu) + S_{1,0} \mathcal{G}^{\sigma}_{\mathcal{L}}(z_\mu) S_{0,1} g^{\sigma}_{1,N}(z_\mu)\\
&\times S_{0,1} \mathcal{G}^{\sigma}_{\mathcal{R}}(z_\mu) S_{1,0} g^{\sigma}_{N,1}(z_\nu) - S_{0,1} g^{\sigma}_{1,N}(z_\mu) S_{0,1} \mathcal{G}^{\sigma}_{\mathcal{R}}(z_\mu)\\
&\times S_{1,0} g^{\sigma}_{N,1}(z_\nu) S_{1,0} \mathcal{G}^{\sigma}_{\mathcal{L}}(z_\nu) - S_{1,0} \mathcal{G}^{\sigma}_{\mathcal{L}}(z_\mu) S_{0,1} g^{\sigma}_{1,N}(z_\mu)\\
&\times S_{0,1} \mathcal{G}^{\sigma}_{\mathcal{R}}(z_\nu) S_{1,0} g^{\sigma}_{N,1}(z_\nu)\}.
\end{aligned}
\tag{A17}
$$

Using the cyclic invariance of the trace yields

$$
\begin{aligned}
T^{\sigma}(E) = \frac{1}{2}\sum_{\mu,\nu} (-1)^{\mu+\nu} \mathrm{tr}\{ & S_{1,0}[\mathcal{G}^{\sigma}_{\mathcal{L}}(z_\mu) - \mathcal{G}^{\sigma}_{\mathcal{L}}(z_\nu)] S_{0,1} g^{\sigma}_{1,N}(z_\mu) S_{0,1} [\mathcal{G}^{\sigma}_{\mathcal{R}}(z_\mu)\\
&- \mathcal{G}^{\sigma}_{\mathcal{R}}(z_\nu)] S_{1,0} g^{\sigma}_{N,1}(z_\nu)\},
\end{aligned}
\tag{A18}
$$

which is already equivalent to Eq. (9) because the terms $\mu=\nu$ are zero and only terms $\mu\neq\nu$ contribute.

The transmission coefficient consists of two terms

$$
T^{\sigma}(\mathbf{k}_\parallel, E) = \frac{1}{2}[T^{\sigma}_1(\mathbf{k}_\parallel, E) + T^{\sigma}_2(\mathbf{k}_\parallel, E)], \tag{A19}
$$

$$
\begin{aligned}
T^{\sigma}_1(\mathbf{k}_\parallel, E) = \lim_{\delta\to 0+} \mathrm{Tr}\{ & B^{\beta,\sigma}_1(\mathbf{k}_\parallel, E) g^{\beta,\sigma}_{1,N}(\mathbf{k}_\parallel, z_+)\\
&\times B^{\beta,\sigma}_N(\mathbf{k}_\parallel, E) g^{\beta,\sigma}_{N,1}(\mathbf{k}_\parallel, z_-)\},
\end{aligned}
\tag{A20}
$$

$$
\begin{aligned}
T^{\sigma}_2(\mathbf{k}_\parallel, E) = \lim_{\delta\to 0+} \mathrm{Tr}\{ & B^{\beta,\sigma}_1(\mathbf{k}_\parallel, E) g^{\beta,\sigma}_{1,N}(\mathbf{k}_\parallel, z_-)\\
&\times B^{\beta,\sigma}_N(\mathbf{k}_\parallel, E) g^{\beta,\sigma}_{N,1}(\mathbf{k}_\parallel, z_+)\},
\end{aligned}
\tag{A21}
$$

related by the identity

$$
T^{\sigma}_1(\mathbf{k}_\parallel, E) = T^{\sigma}_2(-\mathbf{k}_\parallel, E). \tag{A22}
$$

Consequently, $T^{\sigma}(-\mathbf{k}_\parallel, E) = T^{\sigma}(\mathbf{k}_\parallel, E)$, and therefore

$$
\begin{aligned}
\sum_{\mathbf{k}_\parallel}^{\mathrm{SBZ}} T^{\sigma}(\mathbf{k}_\parallel, E) &= \sum_{\mathbf{k}_\parallel}^{\mathrm{SBZ}} T^{\sigma}_1(\mathbf{k}_\parallel, E) = \sum_{\mathbf{k}_\parallel}^{\mathrm{SBZ}} T^{\sigma}_2(\mathbf{k}_\parallel, E)\\
&= 2\sum_{\mathbf{k}_\parallel}^{\Omega} T^{\sigma}(\mathbf{k}_\parallel, E).
\end{aligned}
\tag{A23}
$$

The last sum is confined to one-half of the surface Brillouin zone Ω ($\mathrm{SBZ} = \Omega \cup \hat{\mathrm{I}}\Omega$, where $\hat{\mathrm{I}}$ is the operator of spatial inversion). By using Eq. (A23) one can speed up the calculation of conductance.

[1] M. N. Baibich, J. M. Broto, A. Fert, F. Nguyen Van Dau, F. Petroff, P. Etienne, G. Creuzet, A. Friedrich, and J. Chazelas, Phys. Rev. Lett. **61**, 2472 (1988); G. Binasch, P. Grünberg, F. Saurenbach, and W. Zinn, Phys. Rev. B **39**, 4828 (1989).

[2] W. P. Pratt, Jr., S.-F. Lee, J. M. Slaughter, R. Loloee, P. A. Schroeder, and J. Bass, Phys. Rev. Lett. **66**, 3060 (1991).

[3] P. M. Levy, Solid State Phys. **47**, 367 (1994).

[4] C. Vouille, A. Barthélémy, F. Elokan Mpondo, and A. Fert, Phys. Rev. B **60**, 6710 (1999).

[5] K. M. Schep, P. J. Kelly, and G. E. W. Bauer, Phys. Rev. B **57**, 8907 (1998).

[6] M. A. M. Gijs and G. E. W. Bauer, Adv. Phys. **46**, 285 (1997).

[7] P. Zahn, I. Mertig, M. Richter, and H. Eschrig, Phys. Rev. Lett. **75**, 2996 (1995).

[8] D. R. Penn and M. D. Stiles, Phys. Rev. B **59**, 13 338 (1999).

[9] W. H. Butler, X.-G. Zhang, D. M. C. Nicholson, and J. M. MacLaren, Phys. Rev. B **52**, 13 399 (1995).

[10] P. Weinberger, P. M. Levy, J. Banhart, L. Szunyogh, and B. Újfalussy, J. Phys.: Condens. Matter **8**, 7677 (1996); C. Blaas, P. Weinberger, L. Szunyogh, P. M. Levy, and C. B. Sommers, Phys. Rev. B **60**, 492 (1999).

[11] S. Datta, *Electronic Transport in Mesoscopic Systems* (Cambridge University Press, Cambridge, 1995).

[12] I. Turek, V. Drchal, J. Kudrnovský, M. Šob, and P. Weinberger, *Electronic Structure of Disordered Alloys, Surfaces and Interfaces* (Kluwer, Dordrecht, 1997).

[13] P. Bruno, H. Itoh, J. Inoue, and S. Nonoyama, J. Magn. Magn. Mater. **198-199**, 46 (1999).

[14] E. Yu. Tsymbal and D. G. Pettifor, Phys. Rev. B **58**, 432 (1998).

[15] S. Sanvito, C. J. Lambert, and J. H. Jefferson, Phys. Rev. B **60**, 7385 (1999).

[16] J. A. Støvneng and P. Lipavský, Phys. Rev. B **49**, 16 494 (1994).

[17] J. Mathon, A. Umerski, and M. Villeret, Phys. Rev. B **55**, 14 378 (1997).

[18] J. Cerdá, M. A. Van Hove, P. Sautet, and M. Salmeron, Phys. Rev. B **56**, 15 885 (1997).

[19] S. Sanvito, C. J. Lambert, J. H. Jefferson, and A. M. Bratkovsky, Phys. Rev. B **59**, 11 936 (1999).

[20] P. Weinberger, Philos. Mag. B **75**, 509 (1997).
[21] V. Drchal, J. Kudrnovský, and I. Turek, Comput. Phys. Commun. **97**, 111 (1996).
[22] F. James, Comput. Phys. Commun. **60**, 329 (1990).
[23] V. Drchal, J. Kudrnovský, I. Turek, and P. Weinberger, Phys. Rev. B **53**, 15 036 (1996).
[24] J. Mathon, Phys. Rev. B **55**, 960 (1997).
[25] P. M. Levy and S. Zhang, Phys. Rev. Lett. **79**, 5110 (1998).
[26] G. Tatara, Y.-W. Zhao, M. Muñoz, and N. García, Phys. Rev. Lett. **83**, 2030 (1999).
[27] J. B. A. N. van Hoof, K. M. Schep, A. Brataas, G. E. W. Bauer, and P. J. Kelly, Phys. Rev. B **59**, 138 (1999).
[28] P. Bruno, Phys. Rev. Lett. **83**, 2425 (1999).
[29] S. Zhang and P. M. Levy, Phys. Rev. B **57**, 5336 (1998).
[30] B. L. Gyorffy and G. M. Stocks, in *Electrons in Disordered Metals and at Metallic Surfaces*, Vol. 42 of *NATO Advanced Study Institute Series B: Physics*, edited by P. Phariseau, B. L. Gyorffy, and L. Scheire (Plenum Press, New York, 1979).
[31] O. K. Andersen, O. Jepsen, and D. Glötzel, in *Highlights of Condensed-Matter Theory*, edited by F. Bassani, F. Fumi, and M. P. Tosi (North-Holland, New York, 1985), p. 59.
[32] S. K. Bose, O. Jepsen, and O. K. Andersen, Phys. Rev. B **48**, 4265 (1993).
[33] H. Tanaka and M. Itoh, Phys. Rev. Lett. **81**, 3727 (1998).
[34] I. Turek, J. Kudrnovský, V. Drchal, and P. Weinberger (unpublished).
[35] P. A. Lee and D. S. Fisher, Phys. Rev. Lett. **47**, 882 (1981).
[36] E. M. Godfrin, J. Phys.: Condens. Matter **3**, 7843 (1991).